Optimization of the Flow Schemes in Radiant Recuperators

Rade Karamarković[1,*], Vladan Karamarković[1], Miloš Nikolić[1], Nenad Stojić[1], Miljan Marašević[1]
[1]Faculty of Mechanical and Civil Engineering in Kraljevo/Department for Thermal Technique and Environment Protection, University of Kragujevac, Kraljevo (Serbia)

In glass production and metallurgical processes, radiant recuperators are used to preheat combustion air by heat exchange with high temperature flue gases. For these recuperators, the most popular is concurrent flow arrangement, which compared to other solutions has the lowest interface temperature and the longest lifetime. Compared with concurrent, radiant countercurrent recuperators have only one drawback: the interface temperature is higher at the flue gas entrance. Their comparative advantages are: lower average interface temperature, higher efficiency and smaller pressure drop. Compared with pure concurrent and countercurrent radiant recuperators, designs with double air annulus are slightly more efficient and have a bit smaller interface temperatures, whereas cost and pressure drop are their disadvantages. In the paper, all these four flow configurations are combined by the division of airflow and by the use of different airflow schemes. The improved design is a combination of a countercurrent and a concurrent radiant recupreators. Depending on the geometry, there is an optimal airflow division in the combined recuperator. For the analysis, a cell modeling method validated on a 15 m high, concurrent radiant recuperator used in a glass fiber production process is used. Different solutions are analyzed comparing their effectiveness, energy and exergy efficiencies, and interface temperatures.

Keywords: Radiant recuperator, Heat transfer, Cell modelling method, Effectiveness, Double annulus, Flow division

1. INTRODUCTION

Flue gases leaving metallurgical and glass production furnaces contain highly valuable sensible heat. In glass fiber production, flue gas exit temperatures higher than 1200 °C are usual [1]. Thermodynamically, the preferable use of high temperature waste heat is for power production, but in these industries, it is economically justified to use this heat to maintain high temperatures of technological processes. This is achieved by recuperators, in which combustion air is preheated by heat exchange with hot flue gases. The use of preheated air increases combustion temperature and the process efficiency [2].

Recuperators are classified according to [3]: (i) their material: metallic or ceramic, (ii) dominant mode of heat transfer: convective, radiant, and combined (convection and radiation) recuperators etc. Two types of radiant recuperators are frequently used [3]: pipe-in-pipe, depicted in Figs. 1 and 2, and tubular of cage type recuperator. In this field the ongoing research spreads in [3,4]: (i) developing new materials and coatings, (ii) developing new designs, (iii) modification and optimization of the existing designs, and (iv) mathematical modelling.

Compared with concurrent, radiant countercurrent recuperators have only one drawback: the interface temperature is higher at the flue gas entrance. Their comparative advantages are: lower average interface temperature, higher efficiency and smaller pressure drop [4]. The lowest interface temperature produces the longest useful, life-time for a recuperator, and is the main reason why concurrent arrangement is the most popular for recuperators [5]. Compared with pure concurrent and countercurrent radiant recuperators, designs with two air annuluses (see Fig. 2 (e), and (f)) are slightly more efficient and have a bit smaller interface temperatures, whereas cost and pressure drop are their disadvantages. Table 1 shows the recommendations for air and flue gas velocities depending on the design of pipe-in-pipe radiant recuperator [4,6].

Table 1. Recommended velocities of flue gas and air depending on the design of radiant recuperators. The designs are depicted in Fig.2 (c) – (f).

	Pipe-in-pipe	Double pipe-in-pipe
Flue gas [m/s]	3-5 [6]	3-5 [4]
Air [m/s]	20-30 [6]	in the outer annulus <2 [4] in the inner annulus 25-30 [4]

The purpose of the paper is to solve the problem of high interface temperatures in countercurrent radiant recuperators without a noticeable decrease of its efficiency by the division of air flow or by the use of different air flow arrangements. Figure 3 shows the examined arrangements. Figure 3 (a) depicts a combined recuperator obtained by the division of air flow. This design distinguishes two different sections and presents combination of a countercurrent and a concurrent heat exchanger. The aim is to unite positive features of both designs. At the flue gas entrance into the recuperator, one air stream flows concurrently to the gas. On the opposite end, the other air stream flows countercurrently to the flue gas. Figure 3. (b) depicts a double pipe-in-pipe (double annulus) configuration, which is similar to the one shown in Fig. 3 (a). The difference is that the air firstly flows through outer and then through the inner annulus. Fig. 3 (c) shows the air flow arrangement without the separation of the air flow. This arrangement also has two different sections. At the entrance of the flue gas, there is a double annulus with a concurrent air flow to the flue gas that flows through the central pipe and a countercurrent flow of the air in the outer annulus to the air in the inner annulus. The air leaving this part of the recuperator than enters into the other part, which has opposite flow configuration. The proposed designs are not a novelty. They have been reported in [5,7] but they have not been thermodynamically analyzed and compared.

*Corresponding author: Dositejeva 19, 36000 Kraljevo, Serbia, karmarkovic.r@mfkv.kg.ac.rs

The basis for the analyses is a 15 m high recuperator used downstream of a glass fiber kiln, which is shown in Figs. 1 and 2. It is a concurrent pipe-in-pipe radiant heat exchanger in which both fluids: flue gas and combustion air, enter from the bottom and exit at the top. Flue gas flows through the central pipe and combustion air flows through the annulus, which is shown in Fig. 2 a) and b). The annulus has fins over the perimeter of the outer surface of the inner cylinder. These fins are placed over the entire annulus length. They influence the heat transfer but are placed primarily to facilitate assemblage, secure the distance between the cylinders, and prevent buckling and bulging of the innermost cylinder. The structure hangs supported from the above, which means that the maximum load on the material is at the top of the recuperator. To secure material strength in this zone a cooling air is introduced just above the combustion air exit, as can be seen in Fig. 1. The examined recuperator is built from high temperature resistant chrome nickel steel.

The tool for the analysis is a cell modelling method described and validated in [4]. Four different cells enable modelling of all examined flow configurations.

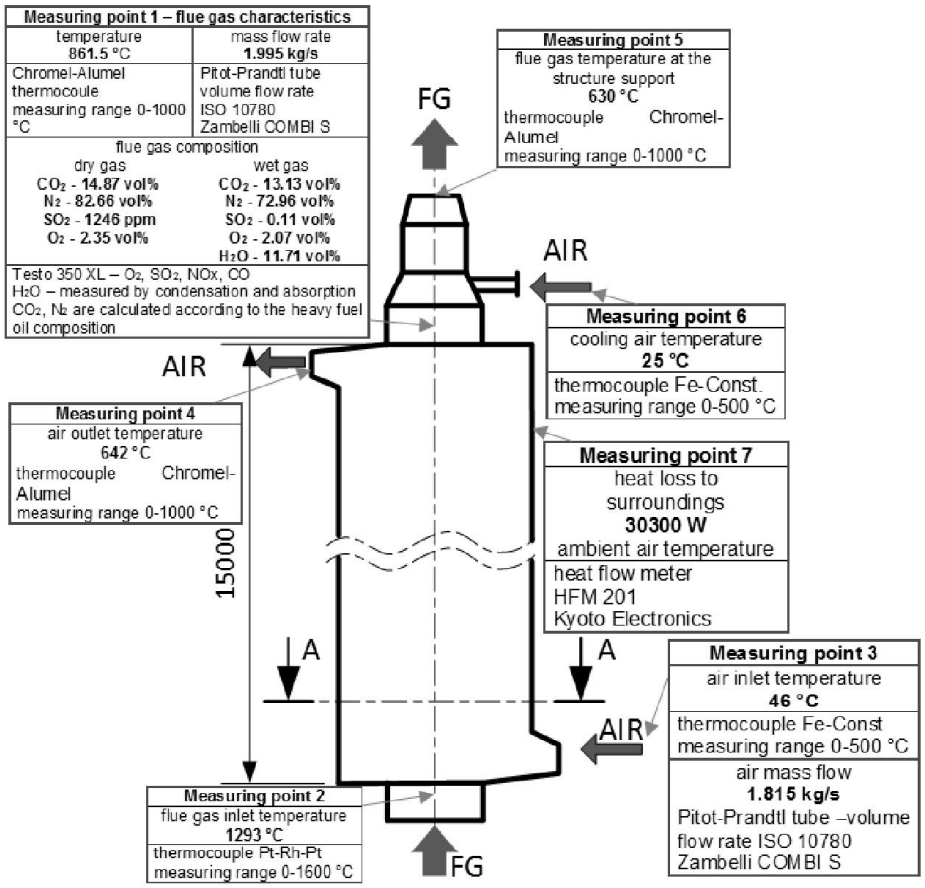

Figure 1: Measuring points, instruments, and results for the examined radiant recuperator.

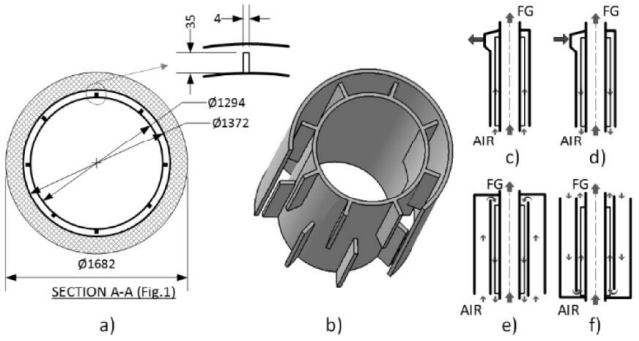

Figure 2: (a) cross section A-A from Fig. 1 of the examined recuperator with the detail of fins, (b) annular air passage, (c) pipe-in-pipe concurrent, (d) pipe-in-pipe countercurrent, (e) double pipe-in-pipe countercurrent, (f) double pipe-in-pipe concurrent recuperator.

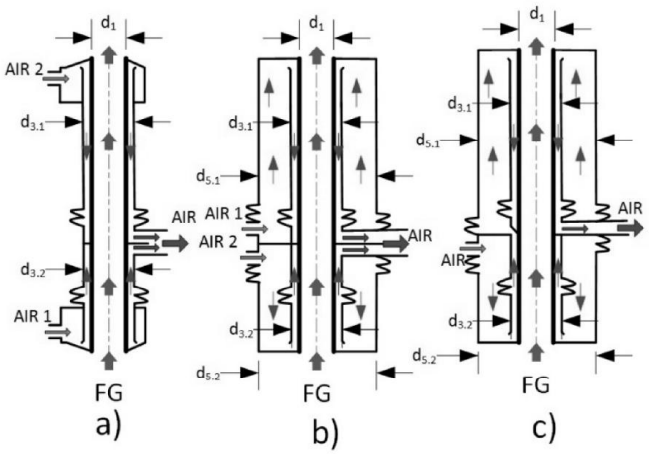

Figure 3: Examined recuperators: (a) combined pipe-in-pipe recuperator, (b) combined double pipe-in-pipe recuperator, (c) combined flow arrangement.

2. MASS AND ENERGY BALANCE OF THE EXAMINED RECUPERATOR

Figure 1 shows the mass and energy balances of the examined recuperator. The balances are obtained after 12 hours of examination by combining average measurement values and calculations.

The recuprator is used to preheat air, here at 642°C, for the combustion of heavy fuel oil in a continuous glass furnace. The recuperative furnace produces 669.12 kg/h of glass fiber by the use of 970.03 kg/h or raw material. The temperatures in the furnace are kept in the range from 1298 to 1580 °C by the use of side burners. The flue gas, whose composition is given in Fig. 1, leaves the furnace at 1293 °C. Gravity drives molten glass out of the furnace.

In the figure, the measuring devices are given, too. The relative errors of the measured quantities are: for O2 ±0.8%, SO2 ±5%, H2O ±3%, volume flow rates ±3%, and for temperatures less than ±0.5%. The presented values are in agreement with [1].

3. MODEL

The applied model is explained and validated in [4]. Figure 4 shows the structure of the applied heat transfer model. The heat exchanger is divided into a finite number of area elements over which the two fluid streams flow. In this, so-called cell modelling method, a heat exchanger is represented by a system of interconnected but not overlapping cells. The application of this concept gives insight into the interior of a heat exchanger. The concept also allows representation of a stream with a single cell. There are three types of cells in the model, for: flue gas, air, and insulation. Additionally, there are two types of air cells: with and without fins.

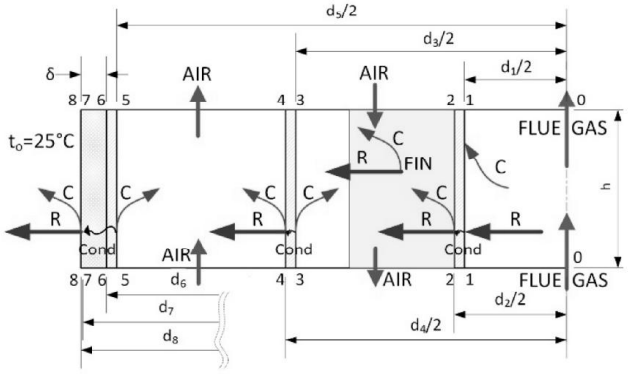

Figure 4: The structure and the principle of the applied cell modeling method.

The first assumptions made in developing the model is that the problem of fluid flow and heat transfer is symmetrical to the central axis of the innermost pipe through which flue gas flows. In Fig. 4, the flue gas cell is limited by the rectangle 0-0-2-2. High temperature flue gas flowing through a pipe is cooled down by convection and radiation. The energy balance for the flue gas in the i-th cell is

$$\dot{m}_{\mathrm{FG}} c_{p_{\mathrm{FG}}}\Big|_{T_{\mathrm{in,FG}_i}}^{T_{\mathrm{out,FG}_i}} \left(T_{\mathrm{in,FG}_i} - T_{\mathrm{out,FG}_i}\right) = \dot{Q}_{\mathrm{con,FG}_i} + \dot{Q}_{\mathrm{rad,FG}_i}, \quad (1)$$

where, $\dot{m}_{\mathrm{FG}} = 1.995$ kg/s is the mass flow rate, c_P in J/kg is the average heat capacity between the inlet $T_{\mathrm{in,FG}}$ and the outlet $T_{\mathrm{out,FG}}$ temperature of the flue gas in the i-th cell. The first term on the right side of Eq. (1) is the convective heat flow rate $\dot{Q}_{\mathrm{con,FG}}$ in W from the flue gas to the pipe wall in the i-th cell and is calculated by the model presented in [8]. The second term on the right side of Eq. (1), $\dot{Q}_{\mathrm{rad,FG}}$ in W represents the radiative heat transfer rate from the flue gas mixture onto the circumference of the enclosing pipe. The radiative heat transfer is calculated by the model presented in [9]. The heat transfer rate, which the inner wall of the pipe (1-1 in Fig. 4) obtains by the convective and radiative heat transfer rate from the flue gas is transmitted to the outer side of the innermost pipe (2-2 in Fig. 4) by the conduction heat flow rate $\dot{Q}_{\mathrm{cond,FG}}$:

$$\dot{Q}_{\mathrm{cond,FG}_i} = \dot{Q}_{\mathrm{con,FG}_i} + \dot{Q}_{\mathrm{rad,FG}_i} = \frac{T_{\mathrm{w1}_i} - T_{\mathrm{w2}_i}}{\frac{1}{2\pi\lambda_{steel}} \ln\frac{d_1}{d_2}}, \quad (2)$$

where $\lambda_{\mathrm{steel}} = 31$ W/mK is the thermal conductivity for the pipe [10]. The diameters in Eq. (2) are shown in Fig. 4.

The rectangle 2-2-4-4 in Fig. 4 limits the air cell. The air flowing through the concentric annular duct is heated by convective heat transfer rates from the inner (2-2) and the outer cylinder (4-4 in Fig. 3). The energy rate balance for the air flow in the i-th cell is:

$$\dot{m}_{\mathrm{a}} c_{p_{\mathrm{a}}}\Big|_{T_{\mathrm{in,a}_i}}^{T_{\mathrm{out,a}_i}} \left(T_{\mathrm{out,a}_i} - T_{\mathrm{in,a}_i}\right) = \dot{Q}_{\mathrm{con,in}_i} + \dot{Q}_{\mathrm{con,out}_i}, \quad (3)$$

where $\dot{m}_{\mathrm{a}} = 1.815$ kg/s is the mass flow rate of air (see Fig. 1), c_P in J/kg is the average heat capacity between the inlet $T_{\mathrm{in,a}}$ and the outlet $T_{\mathrm{out,a}}$ temperature of the air in the i-th cell. $\dot{Q}_{\mathrm{con,in}}$ in W and $\dot{Q}_{\mathrm{con,out}}$ in W are the convective heat transfer rates from the inner and outer surface of the annulus, respectively. A model given in [11] that calculates the heat transfer in concentric annular ducts for fully developed turbulent flow is used to calculate the heat transfer coefficient, which is used to calculate heat transfer rate in each air cell.

In addition to the air flow energy rate balance Eq. (3), the energy rate balances in W for the outer surface of the inner cylinder Eq. (4) and the inner surface of the outer cylinder Eq. (5) are used (surfaces 2-2 and 3-3 in Fig. 4):

$$\dot{Q}_{\mathrm{cond,FG}_i} = \dot{Q}_{\mathrm{con,in}_i} + \dot{Q}_{\mathrm{rad,in}_i}, \quad (4)$$

$$\dot{Q}_{\mathrm{rad,in}_i} = \dot{Q}_{\mathrm{con,out}_i} + \dot{Q}_{\mathrm{cond,out}_i}. \quad (5)$$

The heat flow rate from the corresponding flue gas cell $\dot{Q}_{\mathrm{cond,FG}}$ is partly transferred by heat convection to the air $\dot{Q}_{\mathrm{con,in}}$ and partly radiated to the outer surface of the annulus $\dot{Q}_{\mathrm{rad,in}}$. The radiated heat is then transferred by heat convection to the air $\dot{Q}_{\mathrm{con,out}}$ and partly transferred to the surroundings or the outer air cell $\dot{Q}_{\mathrm{cond,out}}$ depending on the examined construction.

The radiative heat transfer rate $\dot{Q}_{\mathrm{rad,in}}$ consists of two components, which are calculated by the model presented in [12]. The first component of the radiative heat transfer is from the outer surface of the inner cylinder (surface 2-2 in Fig. 4) to the inner surface of the outer cylinder (3-3) [12]. The other component is from the fins to the inner surface of the outer cylinder (3-3).

The term $\dot{Q}_{\text{cond,out}}$ in Eq. (5) is the heat transfer rate through the outer surface of the air cell, which is calculated in each cell as in Eq. (2)

$$\dot{Q}_{\text{cond,out}_i} = \frac{T_{\text{outw}_i} - \text{T}4_i}{\frac{1}{2\pi\lambda_{\text{steel}}}\ln\frac{d_4}{d_3}}. \quad (6)$$

The heat transfer rate defined by Eq. (6) from all outer air flowing cells is transferred by heat conduction through an insulating layer and then by natural convection $\dot{Q}_{\text{con,loss}}$ and radiation $\dot{Q}_{\text{rad,loss}}$ to the surroundings. These two components define the heat loss $\dot{Q}_{\text{loss}} = \dot{Q}_{\text{con,loss}} + \dot{Q}_{\text{rad,loss}}$. The heat flow rate towards the surroundings by convection is calculated by [13], whereas the radiative heat loss is calculated by [12]. As there are several air cells that are connected to an insulation cell, the temperature at the outer surface of the outermost air-flowing cylinder is determined as the arithmetic mean of the corresponding temperatures for all air cells connected to the insulation cell.

The physical properties of all the quantities in the model are referred to the mean air temperature in the cell. Densities, thermal conductivities, thermal diffusivities, dynamic viscosities, Prandtl numbers and air specific heat capacities and enthalpies are calculated by [14-16]. Specific heat capacities and enthalpies of gas species in the flue gas are calculated by [17].

Each cell is 2.5 m high, except the insulation cell which is 15 m high. The disadvantage of the developed model is the negligence of the radiative heat transfer between cells of the same type. This impact is very small between air cells due to tiny view factors. Oppositely, the view factor between two adjacent flue gas cells is not negligible.

3.1. The effectiveness and exergy efficiency of recuperators

The determination of the outlet temperatures of flue gas and combustion air for a recuperator enables calculating its effectiveness ξ, which is the dimensionless ratio between the actual heat transfer and the maximal possible one in a heat exchanger [18]:

$$\xi = \frac{T_{a,out} - T_{a,in}}{T_{FG,in} - T_{a,in}}. \quad (7)$$

It allows comparison of the analyzed designs. Additionally, exergy efficiency enables the comparison between the analyzed designs. It is defined as the ration between all the exergy flow rates that leave the system (flue gas, heat loss, air) to the exergy flow rates that enters the system (flue gas and air):

$$\psi = \frac{\sum_{out} \dot{E}x}{\sum_{in} \dot{E}x} \quad (8)$$

In Eq. (8) all exergy flow rates are calculated as in [19].

3.2. Flow ratio

The all analyses are performed with the constant air flow of 1.815 kg/s. In designs presented in Fig. 3 a) and b) the flow is divided. The measure of the division is the flow ratio m [-], which is the mass flow rate of air through the countercurrent section $\dot{m}_{cc}$ relative to the total air mass flow $\dot{m}$

$$m = \frac{\dot{m}_{cc}}{\dot{m}}. \quad (9)$$

4. RESULTS

The data presented in this section relate to the examined recuperator and its input data (flow rates and inlet temperatures as in Fig. 1). Figure 5 shows what has been stressed in the introduction section, compared with the pure concurrent radiant recuperator, the countercurrent has a higher interface temperature at the flue gas entrance.

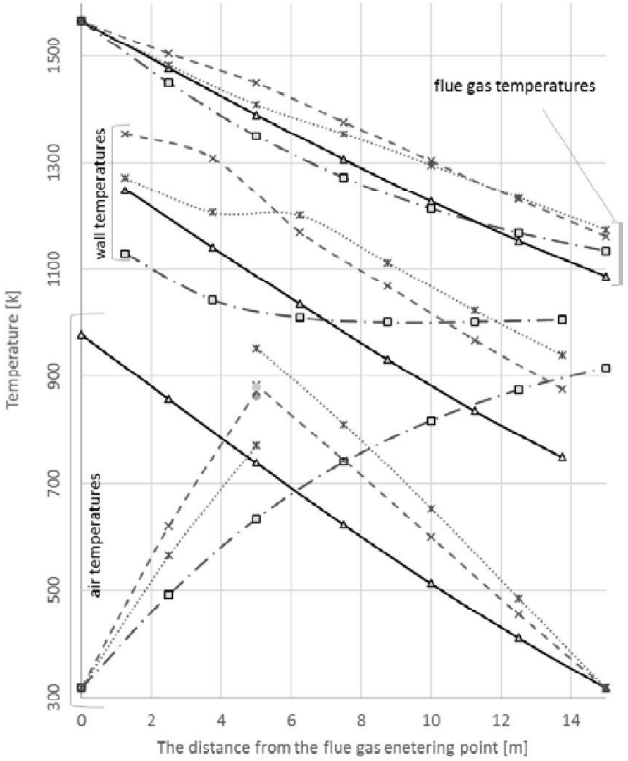

Figure 5: The temperature profiles of flue gas, air and inner surface of the innermost cylinder along the recuperator for different designs that have the same geometry as the experimental recuperator(solid line – countercurrent (Fig. 2 d)), long dash dot line – experimental concurrent (Fig. 2 c)), dash line –combined m=0.7 (Fig. 3 a) d_1=1284 mm, $d_{3.1}$=$d_{3.2}$=1372mm)), dotted line – combined m=0.5).

If the air flow is divided to obtain a combined recuperater, which consists of a concurrent section at the flue gas entrance and a countercurrent section at the flue gas exit, the exit temperature of air is obtained as a mixture of two streams (see Fig 3. a)). The effectiveness, exit temperatures and interface temperatures depend on the flow ratio m if the combined recuperator has the existing dimensions (diameters and fins), which are shown in Figs. 1 and 2, and if the air flow is divided so as the the concurrent and the countercurrent sections are 5 and 10 m long, respectively. The division of the recuperator onto two unequal sections is made based on the interface temperatures for pure concurrent and countercurrent radiant recuperator. These temperatures are shown in Fig. 5. If the existing dimensions are kept, the effectiveness of the combined recuperator is substantially lower than for the existing concurrent recuperator (see Fig. 6). Additionally, maximal interface temperatures are extremely high for

m=0.5 and m=0.7, as it is shown in Fig. 5. The reason for this behavior are the air velocities in the both sections. If the same dimensions are retained as in the existing concurrent recupreator, the temperatures and mass flow rates of air through the sections of the combined recuperator are smaller. Although there are high temperature differences (see Fig. 5) and equal surface areas for the convective heat transfer, the heat flow rate from the flue gas to the air is smaller. Compared to its dependence on temperature difference, the heat transfer coefficient in these annular ducts depends more on air velocity.

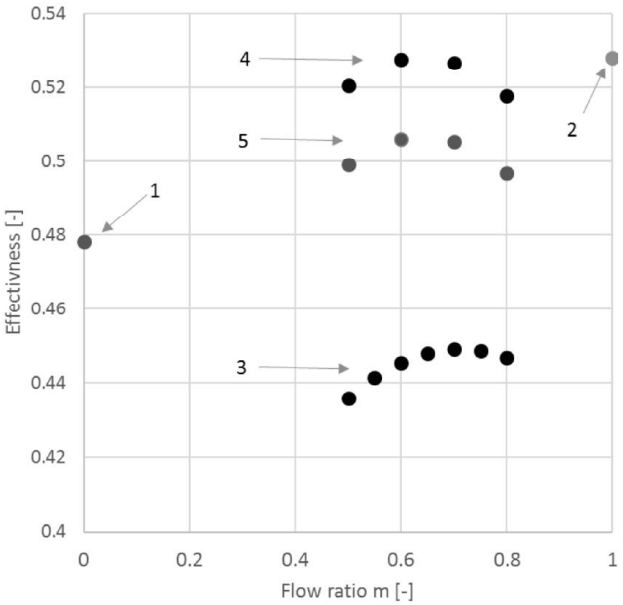

Figure 6: The effectivness for different radiant recuperator desgings; 1 – the existing concurrent recuperator, 2 – the existing countercurrent, 3 – combined (d_1=1284 mm, $d_{3.1}$=$d_{3.2}$=1372mm), 4 – combined (d_1=1284 mm, $d_{3.1}$=1338 (fins 18x4x500mm), $d_{3.2}$=1330 (fins 15x4x500 mm)) , 5 – combined (d_1=1284 mm, $d_{3.1}$=1354 (fins 25x4x500mm), $d_{3.2}$=1334 (fins 15x4x500 mm))

The effectiveness increases if the cross sections of the annuluses decrease (see Fig. 6). This influences the rise of the velocities in both sections of the combined recuperator as can be seen in Fig. 8. However, the cross section of the annulus cannot decrease substantially as it can produce a large pressure drop. Figure 6 shows that for the examined dimensions of combined radiant recuperators, there is an optimal flow ratio. For the recuperator with the existing dimensions the optimal ratio m is around 0.7, whereas for smaller annuluses the optimal ratio is around 0.6.

The combined radiant recuperators, which have an approximately isothermal mixing of two air streams, have the maximal effectiveness. This is shown in Fig. 9, which also depicts the flue gas, wall (interface), and air temperatures across the examined recuperators. For the applied dimensions of air annuluses, the interface temperatures for flow ratio of 0.6 are substantially lower than for the pure countercurrent radiant heat exchanger (see Fig 5.). The reason is a larger temperature difference between the flue gas and the air.

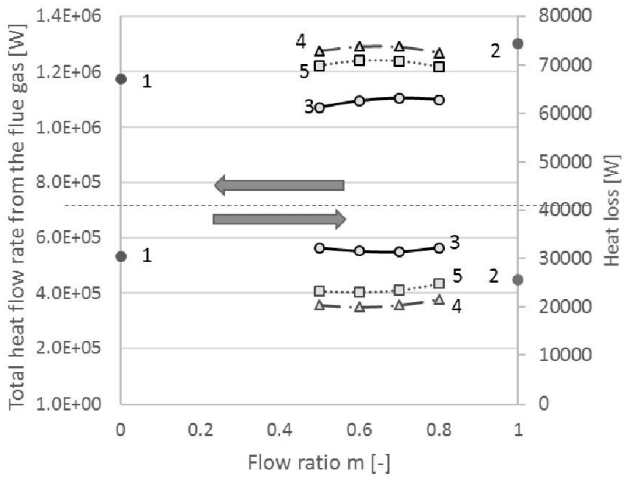

Figure 7: The total heat flow rate from the flue gas and the heat loss depending on the flow ratio m, for different designs: 1 – existing concurrent recuperator, 2 – existing countercurrent, 3 – combined (d_1=1284 mm, $d_{3.1}$=$d_{3.2}$=1372mm (fins 35x4x500)), 4 – combined (d_1=1284 mm, $d_{3.1}$=1338 (fins 18x4x500mm), $d_{3.2}$=1330 (fins 15x4x500 mm)) , 5 – combined (d_1=1284 mm, $d_{3.1}$=1354 (fins 25x4x500mm), $d_{3.2}$=1334 (fins 15x4x500 mm))

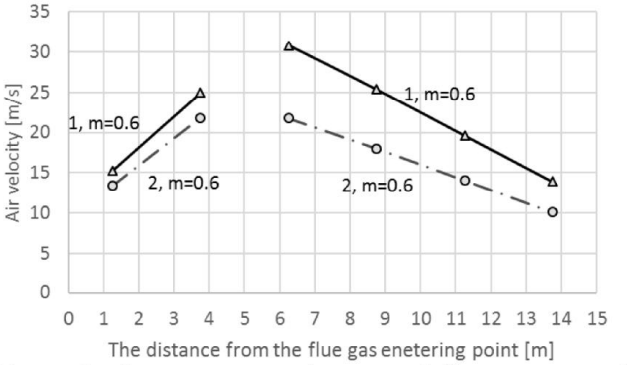

Figure 8: The average air velocities in different sections of the combined recuperator, 1 - d_1=1284 mm, $d_{3.1}$=1338 (fins 18x4x500mm), $d_{3.2}$=1330 (fins 15x4x500 mm) , 2 – d_1=1284 mm, $d_{3.1}$=1354 (fins 25x4x500mm), $d_{3.2}$=1334 (fins 15x4x500 mm)

The combined recuperator with tighter annuluses has larger velocities (see Fig. 8) and consequently a larger average heat transfer coefficient. The temperature profiles along these recuperators are shown in Fig. 9. The figure shows that the most suitable interface temperature have the designs with the largest effectiveness (see Figs. 6 and 7), which have approximately isothermal mixing of two streams.

Figure 7 shows that a lot of different designs of combined recuperator could perform better than the existing concurrent one. Figure 7 also shows the heat losses to the surroundings for the same thickness of insulation applied over the examined designs: 20 cm of mineral wool covered with an aluminum sheet. The differences in heat losses are due to the different air temperatures in air annuluses (the smaller the air temperature the smaller the outer wall temperature) and different outer diameters (the larger the diameter the larger the heat loss).

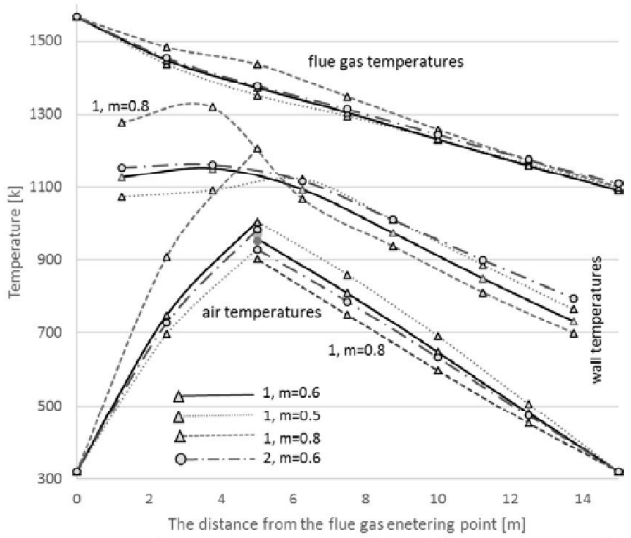

Figure 9: The temperature profiles of flue gas, air and inner surface of the innermost cylinder along the recuperator for different designs of combined recuperator and different flow ratios; 1 and 2 marks the same designs as in Fig. 8.

The application of the second outer annulus over the combined recuperator (double pipe-in-pipe combined design (DC)), with the dimension of the inner annulus as in the existing recuperator, substantially decreases the interface temperature and increases its effectiveness (see Fig. 10 and Tab. 2). Of course, the outer annuls increases the total surface area for the heat transfer. By the variation of all the diameters in this design an improved effectiveness could be obtained.

The smaller interface temperatures could be obtained with a different flow arrangement too. Figure 10 shows this as well. The drawback of the presented CFA design is the pressure drop, which depends on air velocities that are shown in Fig. 11.

Table 2. Properties of the combined double pipe-in-pipe recuperator DC (Fig. 3 b), d_1=1284 mm, $d_{3.1}$=1338 (fins 18x4x500mm), $d_{3.2}$=1330 (fins 15x4x500 mm), $d_{5.1}$=1650, $d_{5.2}$=1450, material thickness 5 mm, m=0.61) and for the combined flow arrangement CFA shown in Fig. 3 c) (d_1=1284 mm, $d_{3.1}$= $d_{3.2}$=1372 (fins as in Fig. 2), $d_{5.1}$=$d_{5.2}$=1550, material thickness 5 mm)

	DC (Fig 3 b))	CFA (Fig 3 c))
Total heat flow rate [MW]	1.30	1.24
Heat loss [W]	20800	19500
Effectivness	0.529	0.507

The exergy efficiency is not suitable for the application on the examined designs, because it is primarily influenced by the flue gas exergy. Compare with the air exergy, the exergy of the flue gas is substantially larger and influences small variations between exergy efficiencies of the examined designs. Nevertheless, for the examined designs the change in exergy is proportional to the change in effectiveness.

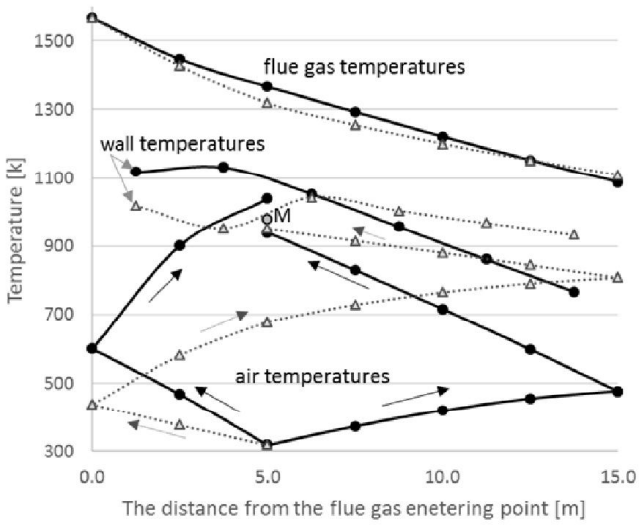

Figure 10: The temperature profiles of flue gas, air and inner surface of the innermost cylinder along the recuperator; solid line – DC recuperator ((Fig 3. b) d_1=1284 mm, $d_{3.1}$=1338 (fins 18x4x500mm), $d_{3.2}$=1330 (fins 15x4x500 mm), $d_{5.1}$=1650, $d_{5.2}$=1450, material thickness 5 mm, m=0.61), dotted line – CFA ((Fig. 3 c) d_1=1284 mm, $d_{3.1}$= $d_{3.2}$=1372 (fins as in Fig. 2), $d_{5.1}$=$d_{5.2}$=1550, material thickness 5 mm)

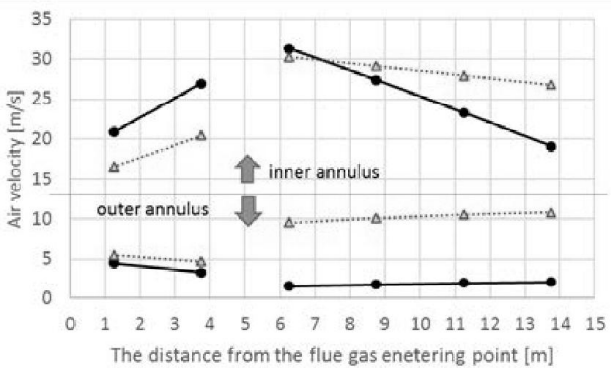

Figure 11: The average air velocities along the DC and CFA recuperators (dimensions are givne in Fig. 10)

5. CONCLUSIONS

From the applied analysis, it can be concluded that the effectiveness of a radiant recuperator could be increased and the interface temperature could be decreased by the implementation of the combined radiant recupeator, double combined recuperator and combined air flow arrangements. The presented solutions sum up comparative advantages of concurrent, countercurrent and double-pipe-in-pipe radiant recuperators.

Depending on the applied geometry, there is an optimal airflow division to concurrent and countercurrent sections of a combined radiant recuperator. For the examined designs, the optimal dimensions should be obtained by an economic analysis. Certainly, designs that are more complex are more expensive. Also, smaller cross section areas of air flow annuluses influence larger heat transfer coefficients and oppositely larger pressure drops.

For all presented solutions (see Fig. 3), the optimal design should have the variable diameters of annuluses along the recuperator.

REFERENCES

[1] http://www.lehigh.edu/imi/teched/GlassProcess/Lectures/Lecture03_Hubert_industglassmeltfurnaces.pdf

[2] Dolianitis, I., *et al.*, "Waste heat recovery at the glass industry with the intervention of batch and cullet preheating," Thermal Science, Vol 20 (4), pp. 1245-1258, (2016)

[3] Sharma, H., *et al.,* "A review of metallic radiation recuperators for thermal exhaust heat recovery", Journal of Mechanical Science and Technology, Vol 28 (3), pp. 1099-1111, (2014)

[4] S. Knežević, R. Karamarković, V. Karamarković, N. Stojić, "Radiant recuperator: modeling and design", Thermal Science, Vol 21 (2), pp. 1119-1134, (2017)

[5] Marnell, C.J., "Development of the radiant recuperator", Proceedings of The first industrial energy technology conference, Houston, TX, April 1979, pp. 607-619, (1979)

[6] Mitov, I., "Comparative analysis of the energy efficiency of metal recuperators with a different design", Journal of the University of Chemical Technology and Metallurgy, Vol. 46 (4), pp. 427-432, (2011)

[7] Meder S.R., White A. J, "Air-cooled radiation recuperator", US Patent No. 3446279 A, (1969)

[8] Gnielinski, V., "Heat Transfer in Pipe Flow", in: VDI Gesellschaft, VDI Heat Atlas, second ed., Springer, Heidelberg (Germany), pp. 693-699, (2010)

[9] Vortmeyer, D., Kabelac, S, "Gas Radiation: Radiation from Gas Mixtures", in: VDI Gesellschaft, VDI Heat Atlas, second ed., Springer, Heidelberg (Germany), pp. 979-989, (2010)

[10] Kozić, Dj., et al., "Handbook for Thermodynamics (Priručnik za termodinamiku)", Faculty of Mechanical Engineering, Belgrade (Serbia), (1995)

[11] Gnielinski, V.," Heat transfer in concentric annular and parallel plate ducts", in: VDI Gesellschaft, VDI Heat Atlas, second ed., Springer, Heidelberg (Germany), pp. 947-959, (2010)

[12] Kablec, S., Vortmeyer, D., "Radiation of surfaces", in: VDI Gesellschaft, VDI Heat Atlas, second ed., Springer, Heidelberg (Germany), pp. 947-959, (2010)

[13] W. Kast, H. Klan, "Heat Transfer by Free Convection: External Flows", in: VDI Gesellschaft, VDI Heat Atlas, second ed., Springer, Heidelberg (Germany), pp. 667-671, (2010)

[14] Kleiber, M., Joh, R., "Calculation methods for thermophysical properties", in: VDI Gesellschaft, VDI Heat Atlas, second ed., Springer, Heidelberg (Germany), pp. 121-152, (2010)

[15] Kleiber, M., Joh, R., "Properties of selected important pure substances", in: VDI Gesellschaft, VDI Heat Atlas, second ed., Springer, Heidelberg (Germany), pp. 153-299, (2010)

[16] Kleiber, M., Joh, R., "Properties of pure fluid substances", in: VDI Gesellschaft, VDI Heat Atlas, second ed., Springer, Heidelberg (Germany), pp. 301-417, (2010)

[17] Balmer, R.T., "*Thermodynamics*", West Publishing Company, ST. Paul, New York, Los Angeles, San Francisco, (USA), (1990)

[18] http://www-unix.ecs.umass.edu/~rlaurenc/Courses/che333/lectures/Heat%20Transfer/Lecture21.pdf

[19] V. Karamarković, M. Marašević, R. Karamarković, M. Karamarković, "Recuperator for waste heat recovery from rotary kilns", Appl. Therm. Eng., Vol. 54 (2), pp. 470-480, (2013).